

The internal electric field originating from the mismatch effect and its influence on ferroelectric thin film properties

This article has been downloaded from IOPscience. Please scroll down to see the full text article.

2004 J. Phys.: Condens. Matter 16 3517

(<http://iopscience.iop.org/0953-8984/16/21/002>)

View [the table of contents for this issue](#), or go to the [journal homepage](#) for more

Download details:

IP Address: 129.252.86.83

The article was downloaded on 27/05/2010 at 14:41

Please note that [terms and conditions apply](#).

The internal electric field originating from the mismatch effect and its influence on ferroelectric thin film properties

M D Glinchuk and A N Morozovska

Institute for Problems of Materials Science, National Academy of Science of Ukraine,
Krjijanovskogo 3, 03142 Kiev, Ukraine

Received 30 January 2004

Published 14 May 2004

Online at stacks.iop.org/JPhysCM/16/3517

DOI: 10.1088/0953-8984/16/21/002

Abstract

The influence of the mismatch effect on thin ferroelectric film properties has been studied in the phenomenological theory framework. The polarization dependent part of the surface energy that defined the boundary conditions for the Euler–Lagrange differential equation was written as a surface tension energy. The latter was expressed via the surface polarization and the tension tensor related to the mismatch of the substrate and film lattice constants and thermal expansion coefficients. The interfacial strain caused by the mismatch effect induces the additional surface polarization P_m via a piezoelectric effect that arises near the surface in any film.

The new parameter P_m/P_S (P_S is the known value of the spontaneous polarization in the bulk ferroelectric material at $T = 0$ K) appeared in the derived phenomenological equations. So we calculate the influence of the parameter P_m/P_S on the depth distribution of the dimensionless film polarization P/P_S , its dependence on temperature, film thickness and applied electric field, as well as that on the hysteresis loop shape, coercive field values, phase diagram and average dielectric susceptibility temperature dependence. Non-zero P_m/P_S values cause a mismatch induced thickness dependent internal electric field E_m . We have shown that this field drastically influences all the properties. In particular, the polarization profile becomes asymmetrical, the polarization temperature dependence resembles that in the external electric field and there is a possibility of external field screening by the internal field E_m . The asymmetry obtained for the hysteresis loop suggests that it is possible that the self-polarization phenomenon recently observed in some films is related to the mismatch effect. The thickness induced ferroelectric–paraelectric phase transition has been shown to exist when $|P_m|/P_S < 1$. A large enough ratio $|P_m|/P_S > 1$ could be the physical reason for the ferroelectric phase conservation in ultrathin film. The possibility of observing the peculiarities of the film property temperature and thickness dependences related to the mismatch effect is discussed.

1. Introduction

The influence of the substrate on ferroelectric thin film properties is known to be related to the appearance of mechanical tension due to mismatch between the lattice constants and thermal expansion coefficients of the film and its substrate as well as growth imperfections. This phenomenon was taken into account by consideration of the uniform mechanical tension tensor u_{ii} ($i = x, y$, when z is the direction normal to the surface). Inclusion of this tensor into the free energy of bulk ferroelectrics, taking into account its coupling to electric polarization via electrostriction in cubic lattices and subsequent minimization of the free energy, has shown [1, 2] lowering of the cubic symmetry to tetragonal symmetry as one could expect for any film and renormalization of free energy coefficients and, so, ferroelectric phase transition temperature. The results obtained are characteristic for bulk ferroelectrics under uniform mechanical tension of the symmetry considered. The effects obtained in [1, 2] were completely independent of the film thickness and so they did not contribute to the size effects of the film properties. The latter are known to be related to the difference between the surface and bulk properties, so the gradient of the polarization appears in the free energy functional, which after variation gives the Euler–Lagrange differential equation with boundary conditions related to the surface energy parameters (see e.g. [3] and references therein). It is obvious that the mechanical tension related to the mismatch effects can contribute to the surface energy and so to the boundary conditions and finally to all the properties of the film. On the other hand, the appearance of misfit dislocations at some critical distance from the film surface, when the appearance of the dislocations becomes energetically preferable, can essentially decrease the mechanical tension inside a thick enough film, taking into account the critical thickness for the appearance of dislocations being several tens or hundreds of nanometres [4, 5]. Therefore for films thinner than the critical thickness for misfit dislocations, the mechanical tension can be considered as a uniform one, while for the thicker films it transforms into a smaller non-uniform tension because of the influence of misfit dislocations. The authors of [4, 5] propose considering the latter effect approximately by substitution of some smaller effective tension for the u_{ii} value, taking into account that for thick enough films the mechanical tension becomes negligibly small.

It is obvious that the mechanical tension effect is the most important for thin enough ferroelectric films and it has to be included both in the surface energy and in the ‘bulk’ part of the free energy functional. In the present work we performed for the first time calculations of the dielectric permittivity, the characteristics of the thickness induced ferroelectric–paraelectric transition and the conditions for its absence, self-polarization and hysteresis loops, by solution of the Euler–Lagrange equation for inhomogeneous polarization with boundary conditions which include the new parameter P_m/P_s originating from the mismatch effect.

2. Model and general formalism

2.1. Free energy functional

Let us consider a ferroelectric thin film with the thickness l ($-l/2 \leq z \leq l/2$) and polarization in the direction z normal to the surface ($P_z \equiv P$). In the phenomenological theory approach the free energy functional can be written in the form [3]

$$\Delta G = G - G_0 = \int g_v dv + \int g_s ds. \quad (1)$$

Here the first and the second integrals reflect the polarization dependent contribution of the bulk and the surface of the film, while G_0 is the polarization independent part of the free energy.

The bulk free energy density g_v can be represented as

$$g_v = \frac{\alpha P^2}{2} + \frac{\beta P^4}{4} + \frac{\delta}{2} \left(\frac{dP}{dz} \right)^2 - P \left(E_0 + \frac{E_d}{2} \right). \quad (2)$$

Here the coefficients α , β are supposed to be renormalized by mechanical tension on the basis of the procedure developed in [1]; E_0 is the external electric field; E_d is the depolarization field and its value for the case of single-domain insulator film with superconducting electrodes can be written in the form [6]

$$E_d = 4\pi(\bar{P} - P). \quad (3)$$

Hereafter a bar over a letter denoting a physical quantity represents spatial averaging over the film thickness. It is seen that in the bulk samples with homogeneous polarization $\bar{P} = P$, the depolarization field is absent ($E_d = 0$), while in the thin films with inhomogeneous polarization, $E_d \neq 0$. It should be noted that equation (2) is suitable for the description of the second-order phase transitions with parameters $\beta > 0$, $\delta > 0$.

Because the surface energy is related to the surface tension [7], it is possible to represent the second term in equation (1) in a form like that in [8]:

$$G_s = \sum_{i=1}^2 \int \mu_i u_{xx}^{(i)} u_{yy}^{(i)} dx dy. \quad (4)$$

Here the parameters μ and u_{jj} ($j = x, y$) are respectively the surface tension coefficient and the strain tensor components; $i = 1, 2$ reflects the contribution of the film's two surfaces.

In what follows we will consider two main contributions to the deformation tensor, namely one considered in [8], related to the surface polarization P_{sur} via the piezoelectric effect that exists even in a cubic symmetry lattice near the film surface, and a second one related to mismatch effects discussed in the introduction. Therefore

$$u_{xx}^{(i)} = u_{xxm}^{(i)} + d_{xxz}^{(i)} P_{zi}^{(i)}, \quad u_{yy}^{(i)} = u_{yyym}^{(i)} + d_{yyz}^{(i)} P_{zi}^{(i)}, \quad (5)$$

where $z_1 = l/2$, $z_2 = -l/2$, d_{jjz} is the coefficient of the piezoelectric effect; u_{jjm} is the tensor of the mechanical strain which is proportional to the difference in lattice constants and thermal expansion coefficients between a substrate and a film as well as to the growth imperfections. In what follows we will consider an epitaxial film with bulk cubic symmetry, e.g. BaTiO₃, PbTiO₃. In such cases $u_{xx}^{(i)} = u_{yy}^{(i)}$ because $d_{xxz}^{(i)} = d_{yyz}^{(i)} \equiv d^{(i)}$, $u_{xxm}^{(i)} = u_{yyym}^{(i)} \equiv u_m^{(i)}$ and so the product $u_{xx}^{(i)} u_{yy}^{(i)}$ in equation (4) can be rewritten as $u_{xx}^{(i)2} = u_m^{(i)2} + 2d^{(i)} u_m^{(i)} P_{zi} + d^{(i)2} P_{zi}^2$, where the first term is independent of the polarization, while the last two terms are governed by the surface free energy. Taking into account equations (2)–(5), the free energy (1) acquires the form

$$\begin{aligned} \Delta G(P) = & \frac{1}{l} \int_{-l/2}^{l/2} dz \left[\frac{\alpha}{2} P^2(z) + \frac{\beta}{4} P^4(z) + \frac{\delta}{2} \left(\frac{dP(z)}{dz} \right)^2 - P(z) E_0 \right] \\ & + \frac{2\pi}{l} \int_{-l/2}^{l/2} dz (P(z) - \bar{P})^2 + \frac{\delta}{2l} \left[\frac{(P(l/2) + P_m^{(1)})^2}{\lambda_1} + \frac{(P(-l/2) + P_m^{(2)})^2}{\lambda_2} \right]. \end{aligned} \quad (6)$$

Hereafter we use the following parameters:

$$\lambda_{1,2} = \frac{\delta}{2\mu_{1,2}d^2}, \quad P_m^{(1,2)} \equiv \frac{u_m^{(1,2)}}{d}. \quad (7)$$

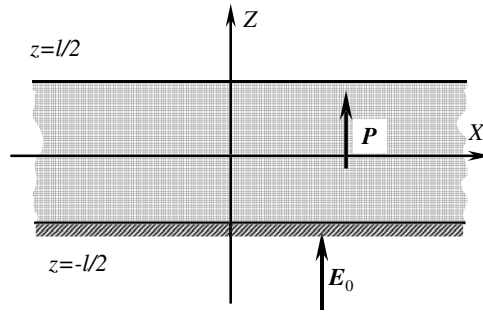


Figure 1. The scheme of the film on the substrate (/////).

Since the signs of the parameters u_m and d can be positive or negative, both $P_m > 0$ and $P_m < 0$ are expected. Because of this we will choose the sign of P_m by comparison with experiment. The extrapolation lengths $\lambda_{1,2}$ can only be positive.

The renormalized coefficient α in (6) has the form [1]

$$\alpha(T) = \alpha_T(T - T_c^*), \quad T_c^* = T_c + \frac{2Q_{12}u_m}{\alpha_T(S_{11} + S_{12})}. \quad (8)$$

Here parameters T_c , α_T , Q_{12} and S_{11} , S_{12} are respectively the ferroelectric transition temperature, inverse Curie constant, electrostriction coefficient and elastic modulus, regarded as known for the bulk material. It follows from the expression for T_c^* in equation (8) that for the given substrate–film pair we can have $T_c^* < T_c$ for $u_m > 0$ or $T_c^* > T_c$ for $u_m < 0$, because $Q_{12} < 0$ for materials with perovskite structure [9]. It should be noted that T_c^* corresponds to the ferroelectric–paraelectric transition temperature of bulk material under compressive or tensile external pressure of the symmetry considered.

2.2. The Euler–Lagrange equation and boundary conditions

The equation for calculation of the polarization can be obtained by variation over the polarization of the free energy functional (6). This yields the following Euler–Lagrange equations and boundary conditions:

$$\alpha P + \beta P^3 - \delta \frac{d^2 P}{dz^2} = E_0 + 4\pi(\bar{P} - P), \quad (9)$$

$$\left(P + \lambda_1 \frac{dP}{dz} \right) \Big|_{z=l/2} = -P_m^{(1)}, \quad \left(P - \lambda_2 \frac{dP}{dz} \right) \Big|_{z=-l/2} = -P_m^{(2)}. \quad (10)$$

In what follows we will consider the realistic situation of a film on a substrate with a free-standing upper surface, where parameter $u_m^{(1)} = 0$ and so $P_m^{(1)} = 0$. To find the transition temperature of the ferroelectric film one has to solve equation (9) with boundary conditions (10) at parameter values $P_m^{(1)} = 0$ and $P_m^{(2)} = P_m \neq 0$ (see figure 1).

Looking for the possibility for obtaining the clearest analytical results, let us solve the linearized equation (9) with equal extrapolation lengths $\lambda_1 = \lambda_2 = \lambda$:

$$\alpha(T)P - \delta \frac{d^2 P}{dz^2} = E_0 + 4\pi(\bar{P} - P), \quad (11a)$$

$$\left(P + \lambda \frac{dP}{dz} \right) \Big|_{z=l/2} = 0, \quad \left(P - \lambda \frac{dP}{dz} \right) \Big|_{z=-l/2} = -P_m. \quad (11b)$$

The solution of (11) has the following form:

$$P_{\text{Lin}}(z) = \frac{E_0 - P_m \Psi(l)/2}{\alpha(T) + \Psi(l)} [1 - \varphi(z)] - \frac{P_m}{2} [\varphi(z) - \xi(z)]. \quad (12)$$

Hereafter we used the following designations:

$$\Psi(l) = 4\pi \left(\frac{2l_d}{l} \right) \frac{th(l/2l_d)}{1 + (\lambda/l_d)th(l/2l_d)}, \quad (13a)$$

$$\varphi(z) = \frac{ch(z/l_d)}{ch(l/2l_d) + (\lambda/l_d)sh(l/2l_d)}, \quad (13b)$$

$$\xi(z) = \frac{sh(z/l_d)}{sh(l/2l_d) + (\lambda/l_d)ch(l/2l_d)}. \quad (13c)$$

The parameter $l_d = \sqrt{\delta/(4\pi + \alpha)}$ is the characteristic length, regarded as known for the bulk material. The expression for \bar{P} can be calculated after taking into account that $\bar{\varphi} = \Psi(l)/4\pi$, $\bar{\xi} = 0$, which leads to

$$\bar{P}_{\text{Lin}}(T, l) = \frac{E_0}{\alpha(T) + \Psi(l)} \left[1 - \frac{\Psi(l)}{4\pi} \right] - \frac{P_m \Psi(l)}{2(\alpha(T) + \Psi(l))} \left[1 + \frac{\alpha}{4\pi} \right]. \quad (14)$$

Notice that $\bar{P}_{\text{Lin}}(T, l)$ diverges at the critical point $\alpha(T) + \Psi(l) = 0$ which is independent of P_m . It was shown earlier in [10, 11] that the origin of this divergence for the films with $P_m = 0$ is the thickness induced ferroelectric–paraelectric phase transition, $\bar{P}_{\text{Lin}}(T, l)$ being the paraelectric phase polarization induced by the external field E_0 . The latter is not true in the case considered, $P_m \neq 0$, as follows from equation (14), so the divergence of $\bar{P}_{\text{Lin}}(T, l)$ cannot indicate the phase transition point. As a matter of fact the second term in equation (14) could be considered as a film self-polarization originating from the mismatch effect. In order to show this, let us make some simplifications in equation (14), taking into account that for most ferroelectrics $l_d \approx \sqrt{\delta/4\pi} \sim 1\text{--}10 \text{ \AA}$ [9] and

$$l \gg l_d, \quad \lambda \gg l_d, \quad \alpha/4\pi \ll 1, \quad (15)$$

so expression (14) can be rewritten as

$$\bar{P}_{\text{Lin}}(T, l, E_0) \approx \frac{E_0 - P_m \Psi(l)/2}{\alpha(T) + \Psi(l)}. \quad (16)$$

It is clear from (16) that the combination $(E_0 - P_m \Psi(l)/2)$ plays the role of the effective field that determines the polarization amplitude. Therefore one has to apply a non-zero external field $E_0 \approx P_m \Psi(l)/2$ in order to compensate for the internal self-polarization induced by the mismatch effect. Possible experimental manifestations of this effect will be discussed later.

Note that the linearization of (9) is valid only for the small polarization amplitudes $|\bar{P}_{\text{Lin}}/P_S| \ll 1$ (hereafter $P_S = \sqrt{\alpha_T T_C^*/\beta}$ is the spontaneous polarization of the bulk material at $T = 0 \text{ K}$), so the results (12), (14) obtained could not be used in the vicinity of the point $T = T_C^*$ where the nonlinear term in equation (9) must be taken into account.

2.3. Free energy with renormalized coefficients

Let us find the approximate solution of the nonlinear equation (9) by the direct variational method [12]. We will choose the one-parametric trial function in the form of a linearized solution (12) that satisfies the boundary conditions (10), namely

$$P(z) = P_V [1 - \varphi(z)] - \frac{P_m}{2} [\varphi(z) - \xi(z)]. \quad (17)$$

The amplitude P_V must be determined by the minimization of the free energy (6). Integration in the expression (6) with the trial function (17) leads to the following form of the free energy:

$$\Delta G(P_V) = \frac{A_m}{2} P_V^2 + \frac{D_m}{3} P_V^3 + \frac{B_m}{4} P_V^4 - P_V[E_0 - E_m]. \quad (18)$$

For validity of the inequalities (15) the renormalized coefficients in (18) have the following form:

$$A_m(T, l) = 4\pi\theta \left(\frac{T}{T_C^*} - 1 + \frac{1}{\theta h(1 + \Lambda)} + \frac{P_m^2}{P_S^2} \frac{(1 + 3\Lambda)}{4h(1 + \Lambda)^3} \right), \quad (19)$$

$$B_m(l) = \beta \left(1 - \frac{11 + 27\Lambda + 18\Lambda^2}{6h(1 + \Lambda)^3} \right), \quad (20)$$

$$D_m(l) = -\frac{\beta P_m}{2h} \left(1 - \frac{\Lambda^3}{(1 + \Lambda)^3} \right), \quad (21)$$

$$E_m(l) = E_S \frac{P_m/P_S}{2h(1 + \Lambda)} \left(\frac{1}{\theta} - \frac{P_m^2/P_S^2}{3(1 + \Lambda)^2} \right). \quad (22)$$

Here the following parameters are introduced:

$$\theta = \frac{\alpha_T T_C^*}{4\pi}, \quad h = \frac{l}{2l_d}, \quad \Lambda = \frac{\lambda}{l_d}, \quad E_S = \alpha_T T_C^* P_S, \quad P_S = \sqrt{\alpha_T T_C^* / \beta}. \quad (23)$$

Note that the odd power P_V^3 in equation (18) is unusual for cubic symmetry perovskite structure ferroelectrics: this term as well as $E_m(l)$ are absent at $P_m = 0$ (see equations (21), (22)); i.e. it is related to the mismatch effect. So all the changes in the renormalized coefficients in comparison with the case of a free-standing film ($P_m = 0$, see [10]) are expressed in terms of the dimensionless parameter P_m/P_S .

3. Polarization and hysteresis loops

The main advantage of the free energy (18) is that it is an algebraic function of P_V , and thus the dependence of $P_V(E_0, T, l)$ can be derived directly from the minimization of the free energy (18) over P_V :

$$A_m(T, l) P_V + B_m(l) P_V^3 + D_m(l) P_V^2 = E_0 - E_m(l). \quad (24)$$

As an example, the zero-field temperature dependence of the polarization $P_V(T, E_0 = 0)$ is depicted in figure 2, where the curves 1 correspond to the condition $P_m = 0$. The temperature dependences represented by curves 1 correspond to those obtained in [10, 11] where $P_V = 0$ at the temperature of the thickness induced ferroelectric–paraelectric phase transition $T = T_{cl}(l)$. The value of $T_{cl}(l)$ decreases with the film thickness h decreasing and $T_{cl}(l) = 0$ at $h \leq 8$, which corresponds to the critical thickness. At $P_m \neq 0$, $E_0 = 0$ the behaviour of $P_V(T, E_0 = 0)$ looks like that in the external field and for the thickest film ($h = 40$) it resembles the behaviour in the bulk samples (see e.g. [9]). To find the physical meaning of the polarization P_V , let us calculate the average polarization. In accordance with (13b), (17), (19) and (23) the average polarization acquires the form

$$\bar{P} = P_V \left[1 - \frac{1}{h(1 + \Lambda)} \right] - \frac{P_m}{2} \frac{1}{h(1 + \Lambda)}. \quad (25)$$

Keeping in mind that for most thin ferroelectric films $h \geq 10$, $\Lambda \geq 10$, one can see that $\bar{P} \approx P_V$.

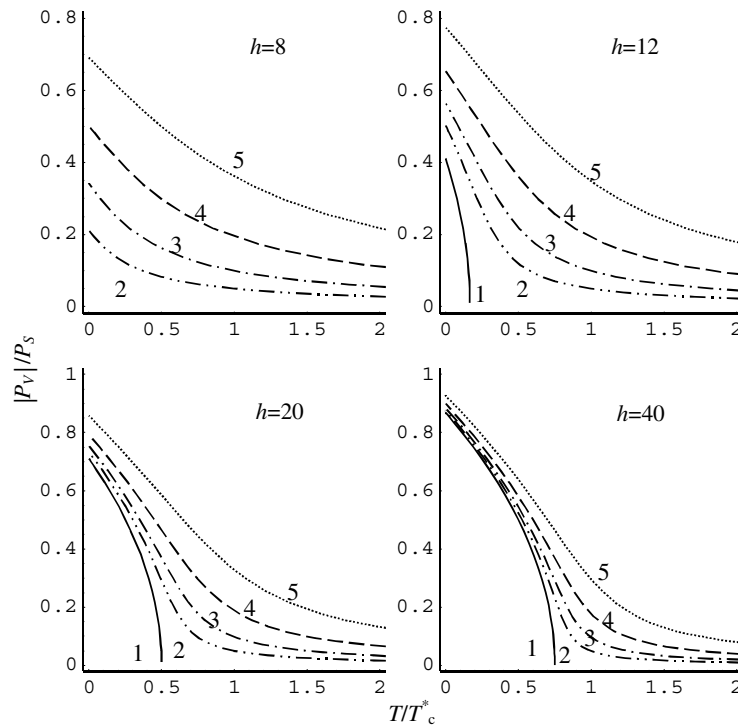


Figure 2. The temperature dependence of the polarization for $\theta = 0.01$, $\Lambda = 10$, $E_0 = 0$ and different P_m/P_S values: 0 (curves 1), 0.1 (curves 2), 0.2 (curves 3), 0.4 (curves 4), 0.8 (curves 5).

The distribution of the ratio $|P(z)|/P_S$ over the coordinate z is represented in figure 3 for several values of the parameter P_m/P_S and $\Lambda = 10$, taking into account the expressions (13b) and (13c) for $\varphi(z)$ and $\xi(z)$ respectively. One can see that at $|P_m/P_S| < 1$ the profiles $P(z)$ look like those obtained earlier for $P_m = 0$ [10, 11], and at $|P_m/P_S| > 1$ a strong asymmetry arises. It originates from the asymmetry of the boundary conditions (11b) caused by the presence of a substrate.

The typical forms of the hysteresis loops $\bar{P}(E_0)$ are represented in figure 4(a). As follows from expression (24) and figure 4(a) the quasi-equilibrium hysteresis loop shifts as a whole along the E_0/E_S axis with P_m/P_S increasing. The right-hand-side shift of the hysteresis loop corresponds to the experimentally observed one [13] in the self-polarized film (compare the form of curve 2 for $h = 40$ in figure 4(a) with the loop in figure 4(b)). Indeed, the authors of [13] came to the conclusion that the shift of the loop is attributable to the natural polarization of more than $50 \mu\text{C cm}^{-2}$ without poling treatment. Because the direction of the shift depends on P_m/P_S sign, hereafter we choose $P_m/P_S > 0$ taking into account the experimental result [13]. Notice that the choice of the sign of P_m/P_S leads to $P_V < 0$ in figures 2, 3. The latter follows from equation (18), because the equilibrium P_V at $E_0 = 0$ has to be negative at $E_m \sim P_m > 0$ (see equation (22)).

The similarity of the calculated and observed hysteresis loops is a point in favour of the statement that the mechanism of the self-polarization phenomenon in thin ferroelectric films could be a mismatch effect. The dependence $\bar{P}(E_0)$ at $P_m = 0$ for the thinnest film ($h = 8$) has the form characteristic for a paraelectric phase. This confirms the above statements that the critical thickness is close to $h = 8$.

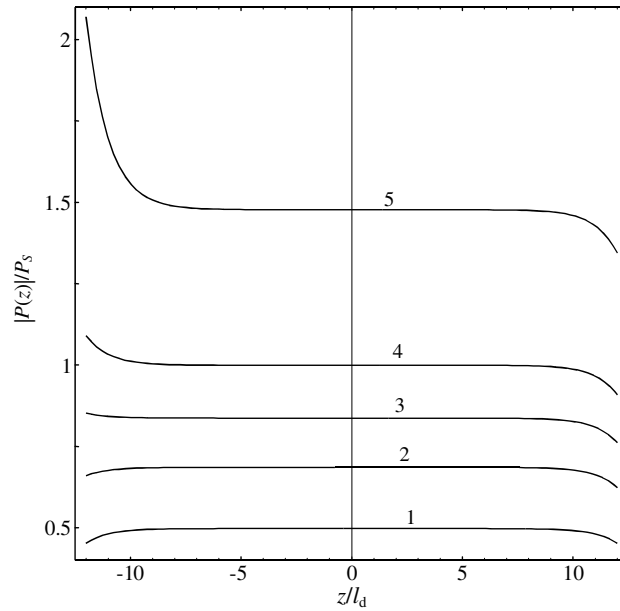


Figure 3. The distribution of the polarization over the coordinate z inside the film for $\Lambda = 10$ and different P_m/P_S values: $P_m/P_S = 0, 0.4, 1, 2, 8$ (curves 1, 2, 3, 4, 5 respectively).

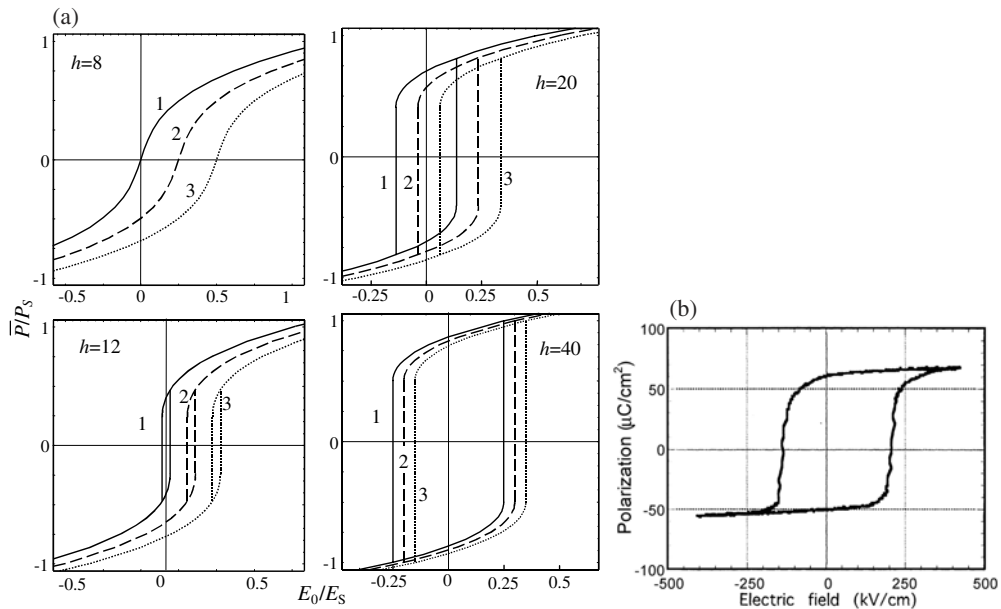


Figure 4. The typical forms of the hysteresis loops $P(E_0)$: (a) theoretical calculation for $\theta = 0.01$, $\Lambda = 10$, $T = 0$ and different P_m/P_S values: 0 (curves 1), 0.4 (curves 2), 0.8 (curves 3); (b) the loop of the PZT film on a MgO substrate [13].

One can see that for the loops depicted in figure 4(a) ($0 < P_m/P_S < 1$) the coercive field increases with film thickness increase. Really, this field can be found from expression (18)

under the condition $d^2\Delta G/dP_V^2|_{P_V=P_{VC}} = 0$ which leads to the equation

$$A_m + 3B_m P_{VC}^2 + 2D_m P_{VC} = 0. \quad (26)$$

The quadratic equation (26) can be easily solved:

$$P_{VC}(T, l) = -\frac{D_m(l)}{3B_m(l)} \pm \sqrt{\left(\frac{D_m(l)}{3B_m(l)}\right)^2 - \frac{A_m(T, l)}{3B_m(l)}}. \quad (27a)$$

Substitution of $P_V = P_{VC}$ into equation (24) yields the exact expression for the coercive field $E_{0C}(T, l)$:

$$E_{0C}(T, l) = E_m(l) - P_{VC}^2[D_m(l) + 2B_m(l)P_{VC}]. \quad (27b)$$

Keeping in mind the inequalities (15), we suppose that parameter P_m/P_S satisfies the conditions

$$\left(\frac{P_m}{P_S}\right)^2 < \frac{3(1+\Lambda)^2}{\theta}, \quad \left(\frac{P_m}{P_S}\right)^2 \ll \frac{4h^2(1+\Lambda)^2}{\theta^2}. \quad (28)$$

Thus equation (27a), when neglecting the term $(D_m(l)/3B_m(l))^2$, can be approximated as follows:

$$P_{VC}(T, l) \approx -\frac{D_m(l)}{3B_m(l)} \pm \sqrt{-\frac{A_m(T, l)}{3B_m(l)}}. \quad (29)$$

On substituting (29) into (27b), with the accuracy $O(D_m(l)/3B_m(l))^2$ one obtains that, in the linear approximation to P_m/P_S ,

$$E_{0C}(T, l) \approx \pm \frac{2}{3} \sqrt{-\frac{A_m^3(T, l)}{3B_m(l)}} + E_m(l) - D_m(l) \frac{A_m(T, l)}{3B_m(l)}. \quad (30)$$

Without a mismatch effect ($P_m = 0$), $D_m = 0$, $E_m = 0$, so

$$P_{VC}(T, l) \approx \pm \sqrt{-\frac{A_m(T, l)}{3B_m(l)}}, \quad E_{0C}(T, l) \approx \pm \frac{2}{3} \sqrt{-\frac{A_m^3(T, l)}{3B_m(l)}}. \quad (31)$$

Substitution of $A_m(T, l)$ from equation (19) into (31) yields the following expression for the coercive field E_{0C} :

$$E_{0C}(P_m = 0, T, h) = \pm \frac{2}{3\sqrt{3}} E_S \sqrt{\left(1 - \frac{T}{T_C^*} - \frac{1}{\theta h(1+\Lambda)}\right)^3}, \quad \frac{T}{T_C^*} < 1. \quad (32)$$

One can see that the third term decreases with h increase, so $E_{0C}(P_m = 0)$ increases with thickness increase. For the parameters used in figure 4(a) ($\theta = 0.01$, $\Lambda = 10$, $T = 0$) analytical expression (32) gives $E_{0C}(P_m = 0, h = 40)/E_S = 0.25$ and $E_{0C}(P_m = 0, h = 20)/E_S = 0.13$; the ratios of these two coercive fields are in good agreement with the results of numerical calculations depicted in figure 4(a) (see curves 1). At $h \rightarrow \infty$ equation (32) transforms into the conventional expression for the coercive field of bulk materials. The formulae (32) make it possible to calculate h_{cr} or T_{cr} corresponding to $E_{0C} = 0$:

$$h_{cr}(P_m = 0, T) = \frac{1}{\theta(1+\Lambda)(1 - T/T_C^*)}, \quad (33)$$

$$T_{cr}(P_m = 0, h) = T_C^* \left(1 - \frac{1}{\theta(1+\Lambda)h}\right).$$

Since $E_{0C} = 0$ at $P_m = 0$ corresponds to the paraelectric phase, h_{cr} or T_{cr} has to be the critical thickness or temperature of the ferroelectric–paraelectric phase transition and equations (33)

coincide completely with the corresponding expressions in [10, 11]. Note that at $P_m \neq 0$ and $h \leq 8$ the hysteresis loop width $\Delta_H(T, l) \approx 4/3\sqrt{-A_m^3(T, l)/3B_m(l)}$ (see equation (30)) is close to zero. However, the absence of the loop does not indicate a paraelectric phase for all P_m/P_S ratios. It may be related to the impossibility of switching the large misfit induced field E_m in a thin film.

Let us now consider the thickness dependence of the coercive field given by equation (30) that takes into account the mismatch effect contribution in the linear approximation to parameter P_m/P_S . Taking into account $E_m \sim 1/h$, $D_m \sim 1/h$ (see equations (21), (22)), the difference ΔE_{0C} between the coercive fields at $P_m \neq 0$ and at $P_m = 0$ has to be inversely proportional to the film thickness h . One can see from figure 4(a) that the ratio $\Delta E_{0C}(h = 40)/\Delta E_{0C}(h = 20) \approx 0.5$, i.e. it is really close to the inverse thickness ratio.

For large enough parameter $P_m/P_S > 1$ one has to take into account nonlinear terms in P_m/P_S in $A_m(T, l)$ and $E_m(l)$, which do not change the dependence of these coefficients on the film thickness h (see equations (19), (22)). Therefore the influence of the mismatch effect decreases with the film thickness increase.

It is evident that the field $E_m(l)$ plays the role of a bias field. It is known that biased ferroelectric hysteresis loops are often observed experimentally (see figure 4(b) and [14, 15]). Using the experimental value of the bias field E_0 that makes the loop symmetrical at $E_0 = E_m$, one can obtain the fitting parameter P_m/P_S with the help of the cubic equation (22). Taking into account the condition $\theta \ll 1$, this equation has the solution $P_m/P_S \approx 2h\theta(1 + \Lambda)E_m/E_S$. The extrapolation length Λ should be obtained from independent measurements, e.g. from the pyroelectric current spectrum [16]. The dependence of the ratio $E_m(h)/E_S$ on the film thickness h is represented in figure 5. It is seen that the internal field increases with thickness decrease and $E_m(h)/E_S \sim 1/h$ (see the inset to figure 5). One can see from equation (24), that the polarization and other properties have to be dependent on the difference $E_0 - E_m(l)$, so screening of the external field E_0 by the internal field E_m can be expected.

4. Dielectric susceptibility and phase diagram

The linear dielectric susceptibility $\chi = dP_V/dE_0|_{E_0=0}$ can be obtained from (24):

$$\chi(T, l) = \frac{1}{A_m + 3B_m P_V^2 + 2D_m P_V} \Big|_{E_0 \rightarrow 0}. \quad (34)$$

Let us find the temperature of susceptibility maximum or divergence— $T_m(l)$ —from the condition $d\chi(T, l)/dT = 0$. The derivative $dP_V(T, l)/dT$ obtained from the equation (24) corresponds to the equilibrium condition $P_V(T_m, l)(E_0 - E_m(l)) \geq 0$. After some elementary transformations (see the appendix) one obtains that the maximum of the static susceptibility must satisfy the conditions

$$P_V^2(T_m, l) = \frac{A_m(T_m, l)}{3B_m(l)}, \quad (35a)$$

$$\chi(T_m, l) = \frac{1}{2(3B_m P_V^2(T_m, l) + D_m(l)P_V(T_m, l))}, \quad (35b)$$

$$4P_V^3(T_m, l) + \frac{D_m(l)}{B_m(l)} P_V^2(T_m, l) = \frac{E_0 - E_m(l)}{B_m(l)}. \quad (35c)$$

It should be underlined that equation (35c) reflects the influence of the external electric field E_0 on the value of T_m . To obtain the expression for $T_m(l, E_0)$ let us make some simplifications in equation (35c). Having used (15), (28), we can neglect the term $D_m(l)P_V^2(T_m, l)/B_m(l)$

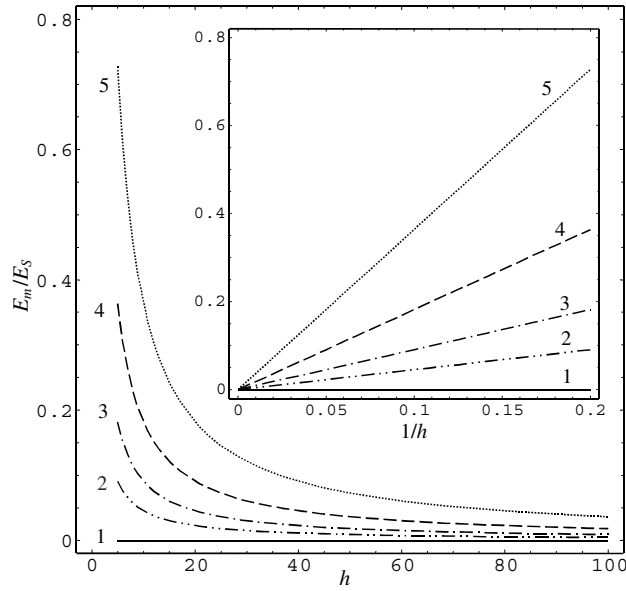


Figure 5. The dependence of the dimensionless internal electric field E_m on the film thickness h for $\theta = 0.01$, $\Lambda = 10$ and different P_m/P_S values: 0 (curve 1), 0.1 (curve 2), 0.2 (curve 3), 0.4 (curve 4), 0.8 (curve 5).

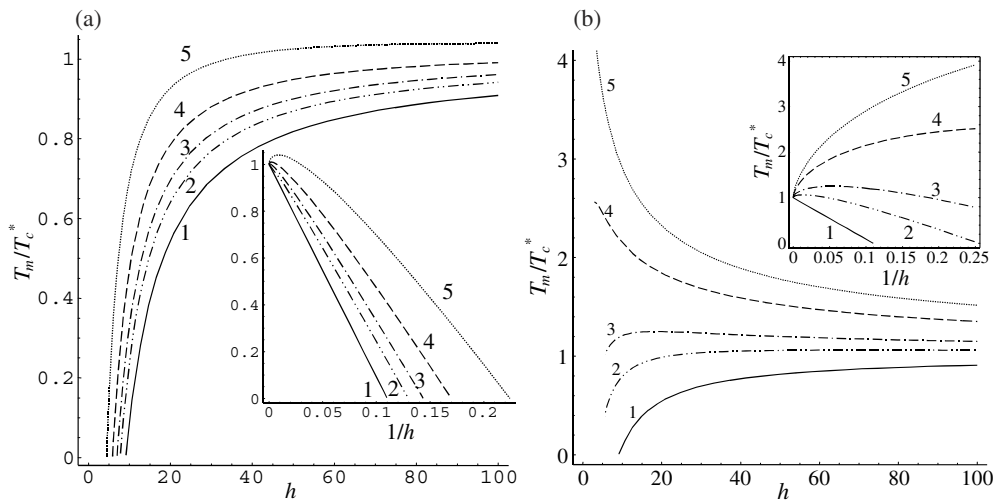


Figure 6. The dependence of the susceptibility maximum temperature T_m on the film thickness h for $\theta = 0.01$, $\Lambda = 10$, $E_0 = 0$ and different P_m/P_S values: (a) 0 (curve 1), 0.1 (curve 2), 0.2 (curve 3), 0.4 (curve 4), 0.8 (curve 5); (b) 0 (curve 1), 1 (curve 2), 2 (curve 3), 5 (curve 4), 8 (curve 5).

in (35c) and obtain that

$$T_m(l, E_0) = T_C^* \left[1 - \frac{1}{\theta h(l)(1 + \Lambda)} + 3 \left(\frac{E_0 - E_m(l)}{4E_S} \right)^{2/3} \right]. \quad (36)$$

Let us put $E_0 = 0$ in equations (22), (36) and obtain that under zero-field conditions

$$T_m(h) = T_C^* \left[1 - \frac{1}{\theta h(1 + \Lambda)} + \frac{3}{4} \left(\frac{P_m/P_S}{\theta h(1 + \Lambda)} \right)^{2/3} \right]. \quad (37)$$

The thickness dependence of the maximum susceptibility temperature $T_m(l)$ is depicted in figure 6, which could be regarded as a phase diagram, taking into account that $T_m(l)$ used to be considered as the temperature of the ferroelectric–paraelectric phase transition. One can see the essential difference between the phase diagrams for $0 < P_m/P_S < 1$ and $P_m/P_S \geq 1$ (compare figures 6(a) and (b)). It follows from figure 6(a) that the critical thickness that corresponds to $T_m = 0$ decreases with the mismatch effect increase; the dependence $(T_m - T_C^*) \sim 1/h$ is in agreement with previous results at $P_m = 0$ [10]. Contrary to this, at $P_m/P_S = 2$ the temperature $T_m \neq 0$ even at $l = 4l_d$, i.e. for ultrathin (close to monolayer) film (see curve 3 in the inset to figure 6(b)). Further increase of the P_m/P_S ratio made $T_m/T_C^* > 1$ for a wide region of the film thickness (see curves 4, 5 in figure 6(b)). Therefore there is no possibility of obtaining $T_m = 0$ for $P_m/P_S > 1$ at any small thickness of a film and so there is no thickness induced ferroelectric–paraelectric phase transition. This could explain the conservation of ferroelectric phase in practically monolayer films, observed earlier (see e.g. [17, 18]). The value $P_m/P_S = 1$ may be considered as a boundary between these two types of behaviour—with and without a thickness induced transition. However, as follows from curve 2 in figure 6(b), for the monolayer film $T_m \approx 0$, so for $P_m/P_S = 1$ the phase transition could exist. For the case $0 \leq P_m/P_S \leq 1$ one can expect anomalies in the dielectric permittivity at the critical temperature or critical thickness.

The maximum linear static susceptibility could be obtained from (35b) and (35c) under the condition of (28) validity as follows:

$$\chi(T_m, l) \approx \frac{1}{3 \sqrt[3]{B_m E_m(l)^2/2}}. \quad (38)$$

One can see from (38) that the susceptibility (34) diverges at $T = T_m(l)$ only if $E_m = 0$, i.e. $P_m = 0$ (see equation (22)). In such a case, $A_m(T_m, l) = 0$ because $A_m(T_m, l) \approx 3/2 \sqrt[3]{B_m E_m(l)^2/2}$ at $E_0 = 0$. Moreover, at $P_m \neq 0$, susceptibility $\chi(T, l)$ only has a maximum at $T = T_m(l)$, which becomes diffuse as the P_m/P_S absolute value increases (see figure 7). It follows from equations (38), (22) that the susceptibility maximum has the view $\chi(T_m, h) \sim h^{2/3} (P_m/P_S)^{-2/3}$, so the maximum becomes sharper and higher with film thickness increase and mismatch polarization decrease. The power law obtained with exponent 2/3 for this behaviour can be checked with the help of experimental data for the film susceptibility dependence on the temperature, film thickness and type of substrate. The analytical expression for the shift of T_m depicted in figure 7, depending on the film thickness and mismatch effect value, is given by equation (37): the shift increases as $C_1 + C_2 (P_m/P_S)^{2/3}$ at fixed thickness and decreases as $C_3 - C_4/h + C_5/h^{2/3}$ at fixed P_m/P_S value. Here $C_{1,2}$ and $C_{3,4,5}$ are constants independent of P_m/P_S and the h values respectively. The observation of the T_m shift can also be useful for checking the validity of the proposed model.

It should be noted that we calculated all the data in figures 2–7 on the basis of exact formulae, while approximate expressions, e.g. (36)–(38), were derived for the sake of illustration.

5. Discussion

The mismatch effect considered in this paper is related to the mechanical strain tensor u_{xx} originating from the difference in substrate and film lattice constants, thermal coefficients and

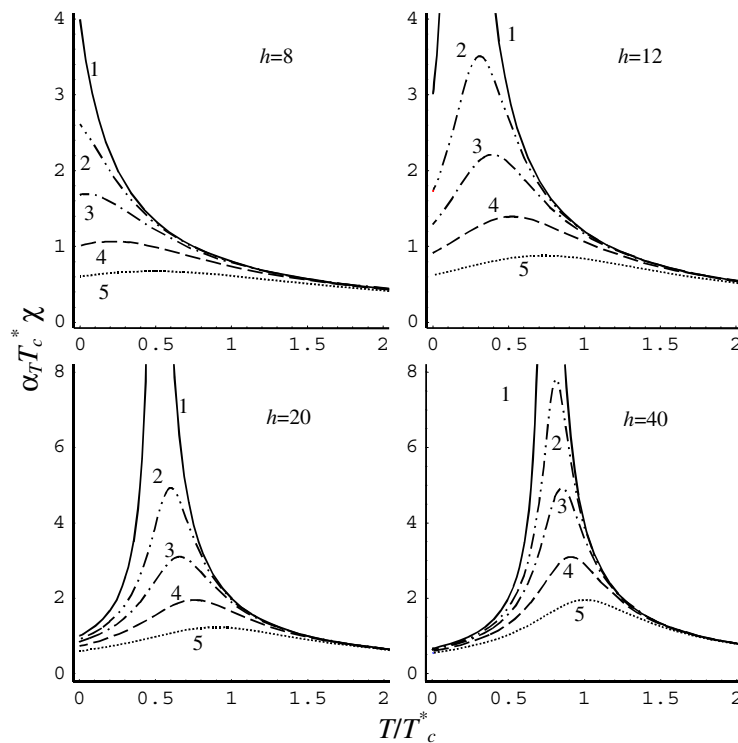


Figure 7. The temperature dependence of the averaged susceptibility for $\theta = 0.01$, $\Lambda = 10$, $E_0 = 0$ and different P_m/P_S values: 0 (curves 1), 0.1 (curves 2), 0.2 (curves 3), 0.4 (curves 4), 0.8 (curves 5).

growth imperfections. The latter depend on the technological process of film fabrication while the others are governed by the substrate–film pair. The mechanical strain influences the electric polarization dependent bulk part of the free energy via electrostriction (see equations (6), (8)) and via the piezoelectric effect on the surface (see equations (4), (5)). The latter effect appears even in cubic lattices because of the absence of an inversion centre in the vicinity of the surface. Because the inversion disappears in the z direction only, while it exists in the x and y ones, the only possible non-zero piezoelectric coefficient related to u_{xx} is $d_{xxz} \equiv d$. As a result, permanent electric polarization on the surface $P_z \equiv P_m$ arises (see equation (7)), while nothing of this kind exists in the x or y directions. Because of this, we supposed that the mismatch effect caused the film self-polarization phenomenon. The shift of the hysteresis loops and the coercive field asymmetry ΔE_{0C} obtained in this paper are known to be characteristic features observed experimentally for self-polarized film (see figure 4(b)).

Since ΔE_{0C} and the coercive field itself are defined essentially by the E_m field, let us estimate its value. To do this we take the following reasonable values of the parameters: $d \sim (10^{-5}–10^{-6})$ CGSE, $\delta \sim (10^{-14}–10^{-16})$ cm², $U_m \sim 10^{-2}$, $\theta \sim 5 \times 10^{-2}$, $l_d \sim 10^{-8}$ cm, $\mu \sim (5–0.5) \times 10^4$ dyn cm⁻², so $P_m = U_m/d \sim (10^3–10^4)$ CGSE and $E_m \approx \frac{4\pi P_m(l_d/l)}{(1+\lambda/l_d)} \sim \frac{l_d/l}{(1+\lambda/l_d)}(10^4–10^5)$ CGSE $\sim \frac{l_d/l}{(1+\lambda/l_d)}3 \times (10^3–10^4)$ kV cm⁻¹. For $l/2l_d \sim 10$ and $\lambda/l_d \sim 10$ one obtains that $E_m \sim (30–300)$ kV cm⁻¹. This is in reasonable agreement with the experimental value $E_{0C} \sim 200$ kV cm⁻¹ obtained for thick enough film (see figure 4(b)). Note that the E_m value obtained shows that this mismatch induced internal field is really able to induce

self-polarization and to screen (at least partially) the external field E_0 in thin ferroelectric films.

On the other hand, the theoretical forecast of $\Delta E_{0C} \sim (P_m/P_S) \cdot 1/h$ obtained here for $|P_m|/P_S < 1$ should be compared with the experimentally observed size effect of coercive field asymmetry (if any) and its dependence on the type of substrate and technological process for self-polarized film. The size effect of the coercive field E_{0C} and its asymmetry ΔE_{0C} for the case $P_m/P_S > 1$, when ferroelectricity remains in ultrathin films [17, 18], was not considered in our paper. Because of this and since at the transition from thin to ultrathin films a change of the switching mechanism from domain nucleation to a homogeneous one (Landau–Khalatnikov) has to be taken into account [19], the size effect is beyond the scope of this paper.

It should be noted that the proposed explanation of the self-polarization phenomenon can be considered as a preliminary one, because more detailed calculations of this phenomenon have to include calculations on the basis of free energy with three components of polarization P_x , P_y and P_z . These calculations are in progress now.

The observation of the other theoretical forecasts, e.g. $\chi(T_m, h) \sim h^{2/3}(P_S/P_m)^{-2/3}$, as well as the peculiar dependence of $\chi(T_m, h, P_m)$ (see figure 7) could be useful for checking the validity of the proposed model, when size effects are related to thickness induced phase transitions, namely, for the cases $|P_m|/P_S < 1$ (i.e. when the polarization induced by the mismatch effect on the surface is smaller than the bulk one). The latter is also valid at $P_m = 0$, because the extrapolation length $\lambda > 0$, as follows from equation (7) because $\delta > 0$, $\mu > 0$. The positive sign of the extrapolation length makes it impossible to explain the reasons for the ferroelectric phase stability in some monolayer films (see e.g. [17, 18]). Our consideration of surface polarization induced by a large enough mismatch effect (the cases of $P_m/P_S > 1$) showed that the physical mechanism of ferroelectric phase conservation for up to one-layer film is the mismatch effect. Experimental confirmation of this statement with different choices of the film–substrate pair is extremely desirable.

Acknowledgment

We are grateful to Professor V M Fridkin for valuable remarks on our paper.

Appendix

Let us find the temperature $T_m(l)$ of the susceptibility maximum or divergence from equation (24) and the condition $d\chi(T, l)/dT = 0$. Taking into account that only A_m and P_V depend on temperature T , we derive that

$$\begin{aligned} \frac{d\chi(T, l)}{dT} &= -\frac{dA_m/dT + (6B_m P_V + 2D_m)dP_V/dT}{(A_m + 3B_m P_V^2 + 2D_m P_V)^2} = 0, \\ \frac{d(A_m P_V + B_m P_V^3 + D_m P_V^2)}{dT} & \\ &\equiv P_V \frac{dA_m}{dT} + (A_m + 3B_m P_V^2 + 2D_m P_V) \frac{dP_V}{dT} = \frac{d(E_0 - E_m)}{dT} \equiv 0. \end{aligned} \quad (\text{A.1})$$

Directly from the system (A.1), one obtains that

$$\begin{aligned} \frac{dP_V}{dT} &= -\frac{dA_m}{dT} \frac{1}{6B_m P_V + 2D_m}, \\ \frac{dP_V}{dT} &= -P_V \frac{dA_m}{dT} \frac{1}{A_m + 3B_m P_V^2 + 2D_m P_V}. \end{aligned} \quad (\text{A.2})$$

The left-hand sides of equations (A.2) are identical; thus from the identity of the right-hand sides we obtain the following equation for $P_V(T_m, l)$:

$$\frac{1}{6B_m P_V + 2D_m} = \frac{P_V}{A_m + 3B_m P_V^2 + 2D_m P_V}. \quad (\text{A.3})$$

From equation (A.3) we obtain $A_m + 3B_m P_V^2 + 2D_m P_V = P_V(6B_m P_V + 2D_m)$ and so

$$P_V^2(T_m, l) = \frac{A_m(T_m, l)}{3B_m(l)}. \quad (\text{A.4})$$

Having substituted (A.4) in the form $A_m(T_m, l) = 3B_m(l)P_V^2(T_m, l)$ into (24) and (34), we immediately obtain equations (35c) and (35b) correspondingly. In contrast, having substituted (A.4) directly into (24), one obtains the equation for $A_m(T_m, l)$, namely

$$\pm 4B_m(l) \left(\frac{A_m(T_m, l)}{3B_m(l)} \right)^{3/2} + \frac{A_m(T_m, l)D_m(l)}{3B_m(l)} = E_0 - E_m(l). \quad (\text{A.5})$$

In accordance with the inequalities (28), the second term in the left-hand side of equation (A.5) can be neglected and then $A_m(T_m, l) \approx \frac{3}{2} \sqrt[3]{B_m(E_0 - E_m(l))^2/2}$. The formulae (37), (38) were derived from the latter expression and equation (19).

References

- [1] Pertsev N A, Zembilgotov A G and Tagantsev A K 1998 *Phys. Rev. Lett.* **80** 1988
- [2] Rossetti G A, Cross L E and Kushida K 1991 *Appl. Phys. Lett.* **59** 2524
- [3] Tilley D R 1996 *Ferroelectric Thin Films, Finite-Size Effects on Phase Transitions in Ferroelectrics* ed C Paz de Araujo, J F Scott and G W Taylor (Amsterdam: Gordon and Breach) pp 11–45
- [4] Speck J S and Pompe W 1994 *J. Appl. Phys.* **76** 466
- [5] Speck J S, Seifert A, Pompe W and Ramesh R 1994 *J. Appl. Phys.* **76** 477
- [6] Kretschmer R and Binder K 1976 *Phys. Rev. B* **20** 1065
- [7] Landau L and Lifshits E 1982 *Statistical Physics Part I* (Oxford: Pergamon)
- [8] Glinchuk M D and Morozovska A N 2003 *Phys. Status Solidi b* **238** 81
- [9] Lines M E and Glass A M 1978 *Principles and Applications of Ferroelectrics and Related Phenomena* (Oxford: Oxford University Press)
- [10] Glinchuk M D, Eliseev E A, Stephanovich V A and Farhi R 2003 *J. Appl. Phys.* **93** 1150
- [11] Glinchuk M D, Eliseev E A and Stephanovich V A 2002 *Physica B* **322** 356
- [12] Dodd R K, Eilbeck J C, Gibbon J D and Morris H C 1984 *Solitons and Nonlinear Wave Equations* (London: Academic)
- [13] Kanno I, Fujii S, Kamada T and Takayama R 1997 *Appl. Phys. Lett.* **70** 1378
- [14] Kholkin A L, Brooks K G, Taylor D V, Hiboux S and Setter N 1998 *Integr. Ferroelectr.* **22** 525
- [15] Pike G E, Warren W L, Dimos D, Tuttle B A, Ramesh R, Lee J, Keramidis V G and Evans J T 1995 *Appl. Phys. Lett.* **66** 484
- [16] Glinchuk M D, Eliseev E A, Deineka A, Jastrabik L, Suchanek G, Sander T, Gerlach G and Hrabovsky M 2001 *Integr. Ferroelectr.* **38** 101
- [17] Ducharme S, Fridkin V M, Bune A V, Palto S P, Blinov L M, Petukhova N N and Yudin S G 2000 *Phys. Rev. Lett.* **84** 175
- [18] Bune A *et al* 1998 *Nature* **391** 874
- [19] Vizdrik G, Ducharme S, Fridkin V and Yudin S 2003 *Phys. Rev. B* **86** 094113